The Radar Cross Section of Small Propellers on Unmanned Aerial Vehicles

Tamás Pető, Sándor Bilicz, László Szűcs, Szabolcs Gyimóthy, József Pávó
Department of Broadband Infocommunications and Electromagnetic Theory
Budapest University of Technology and Economics, Budapest, Hungary,
peto@hvt.bme.hu

***Abstract*—The radar cross section of small-sized unmanned aerial vehicles can be extremely low, making the perception of such objects impossible by standard radar techniques. However, the typical propeller size of these vehicles gives rise to a resonant behavior at some commonly used radar frequency bands. Around the resonant frequency, the radar cross section of the propeller highly depends on the incident wave polarization. Consequently, the rotation of the propeller causes a significant periodic fluctuation of the radar echo, moreover, the propeller length can also be estimated. This phenomenon is studied by means of anechoic chamber measurements and numerical simulations.**

***Index Terms*—UAV, detection, propeller, radar cross section**

I. Introduction

Recently, the Unmanned Aerial Vehicles (UAVs) have got to the focus of attention due to the low construction cost and multifunctionality. This has generated a strong demand for the supervision of these systems by security reasons. However, the detection of small-sized UAVs by means of standard radar techniques is very difficult since they typically have very low Radar Cross Section (RCS). The detailed study of the low probability of intercept flying devices is essential for the development of successful surveillance systems. Exploiting the characteristic features of the reflected signal leads to more robust and sophisticated systems. Many efforts have been made to develop techniques for the radar-based detection of UAVs. A traditional approach to this problem is the application of FMCW or pulse radar based detection technique along with the extraction of the target Doppler signiture to classify tartgets. The opertating frequency of such systems designed to detect small sized targets is typically in the C or X band [1],[2].

In this paper, a promising feature of the rotating propeller of small UAVs in terms of radar-based detection is studied. The propellers of the mini and micro UAVs are commonly made of Carbon-Fiber Reinforced Plastic (CFRP). The electromagnetic properties of this composite material can vary in a wide range, however, at radio frequencies, it can usually be considered as a lossy conductor [3], [4]. Since the typical length of such propellers is around $25\,\mathrm{cm}$, they act similarly to a half-wave dipole antenna around $600\,\mathrm{MHz}$, i.e., in the UHF band, being a typical radar frequency. Consequently, the radar echo backscattered from a propeller is expected to strongly depend on the polarization of the incident wave. Thus, the rotation of the propeller causes a significant fluctuation of the propeller's RCS provided that the excitation frequency is close to the resonant frequency.

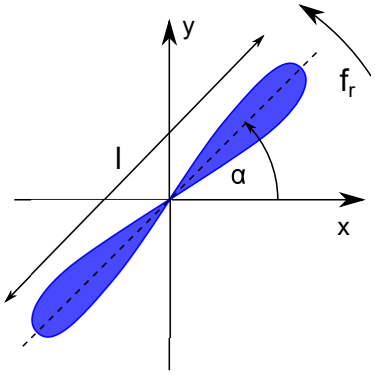

Figure 1. Orientation of the propeller: the rotation plane is the xy plane, the incident wave propagates to the z direction and it is polarized in the x direction.

Let us emphasize that the proposed method definitely differs from the classical micro-Doppler analysis used for the classification of aerial vehicles (including UAVs, [5]). The latter is based on the Doppler frequency shift caused by the rotating blades. In contrary, the present technique is *not* based on the Doppler-shift, it works even if the axis of the rotation points directly towards the radar. Moreover, the micro-Doppler analysis does not account for any resonance phenomenon, this is why it is less sensitive to the applied frequency.

The working principle of the method (Sec. II) is tested by means of both anechoic chamber measurements (Sec. III) and electromagnetic simulations (Sec. IV) as well.

II. Theory

The monostatic radar cross section [6] is given by

$$\sigma = \lim_{r\to\infty} 4\pi r^2 \frac{|E^s(r)|^2}{|E^i|^2} \tag{1}$$

where $|E^i|$ is the amplitude of the electric field strength of the incident plane wave, $|E^s(r)|$ the magnitude of the scattered electric field at distance r from the target. The direction in which $|E^s(r)|$ is evaluated is the same as the direction of arrival of the plane wave, i.e., this scenario models the case of co-located radar transmitter and receiver.

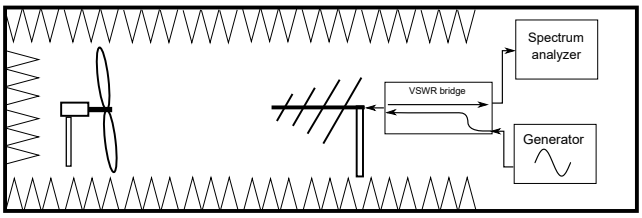

Figure 2. Sketch of the measurement configuration in the anechoic chamber.

Let us consider a propeller made of CFRP, rotating in the xy plane as shown in Fig. 1. Let the direction of arrival of the incident plane wave be the z direction; the incident wave is polarized in the x direction. At those frequencies where the wavelength λ is larger or comparable with the length l, the RCS depends on both the frequency of the excitation f and the orientation of the blades α as well. Provided that the width of the propeller is much smaller than l, the educated guess says that the RCS can be well approximated as

$$\sigma(f,\alpha) \approx \sigma_{\max}(f)\cos^2\alpha = \sigma_{\max}(f)\cos^2 2\pi f_r t \equiv \frac{\sigma_{\max}(f)}{2}(1+\cos 4\pi f_r t) \tag{2}$$

where $\sigma_{\max}(f)$ is the maximal RCS at f and f_r stands for the frequency of the rotation. Consequently, the signal received by the radar will have an amplitude modulated component due to the factor $\cos 4\pi f_r t$ in (2), which results in side-bands at $f \pm 2f_r$ around the carrier frequency. The amplitude of the side-bands is proportional to $\sigma_{\max}(f)$.

Provided that f_r is known or estimated (e.g., by means of adaptive filtering), the radar detection of the rotating propeller is facilitated by the fact that its signature is spectrally separated from the other unwanted echos (clutter).

III. Anechoic chamber measurements

The RCS measurement of a small-sized UAV propeller can be exceedingly difficult even in an anechoic chamber due to its extremely low reflection capabilities. Using the traditional measurement method, the emitted excitation signal and the reflected echo cannot be sufficiently isolated. Moreover, due to the insufficient absorption capabilities of the anechoic chambers, the power level of the sought reflected signal is comparable with (or even lower than) the wall reflections from the absorbing material.

The phenomenon outlined in Sec. II can be exploited not only in a real scenario of UAV detection, but also for the measurement of the propeller's RCS in anechoic chamber.

In our experiment setup, the propeller is rotated by a brushless DC (BLDC) motor and a servo controller (similar to the ones used on a real UAV). The rotation frequency f_r of the propeller is carefully controlled in order to ensure a reproducible measurement. The excitation signal is generated by the RF generator which is connected to a VSWR bridge. The forward port is then connected to the antenna input while the coupled port of the reflected signal is connected to a spectrum analyzer, as sketched in Fig. 2.

Figure 3. The CFRP propeller used for the measurement.

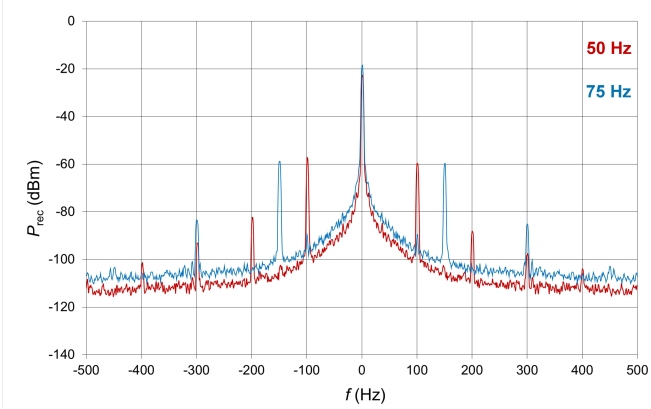

Figure 4. The spectrum of the received signal with two different propeller rotation frequency

The studied propeller (Fig. 3) has a length of $l = 10\,\text{inch}$ and a pitch of $5.8\,\text{inch}$, and it is made of CFRP. As an illustration, the measured spectrum of the received signal for two different rotation frequencies is shown Fig. 4 (shifted to the baseband). The spectrum of the $f_r = 50\,\text{Hz}$ rotation frequency is measured with a transmitted signal $f = 500\,\text{MHz}$ and the spectrum of the $f_r = 75\,\text{Hz}$ rotation frequency is measured with $f = 550\,\text{MHz}$. Let us notice the peaks at the baseband frequencies $f = \pm 2kf_r$ $(k = 0, 1, 2, \dots)$. They can be understood as:

- The center peak $(k = 0)$ is mainly due to the insufficient isolation between the transmitter and receiver channels and to the reflection from the imperfectly absorbing walls of the chamber.
- The first side-peaks $(k = 1)$ correspond to the amplitude modulation of the RCS as discussed in Sec. II, and they are used to calculate the sought $\sigma_{\max}(f)$.
- Further side-peaks $(k \geq 2)$ are due to the higher order harmonics in the RCS with respect to the angle α and to some possible nonlinear distortion in the whole signal processing chain. However, their amplitudes are negligible compared to the $k = 1$ peaks.

Based on the magnitude of the first side-peaks, $\sigma_{\max}(f)$ can be computed, using the radar equation [6]. Without detailing the derivation, the obtained $\sigma_{\max}(f)$ values at 11 excitation frequencies f are plotted in Fig. 5. The maximal RCS is resulted at $550\,\text{MHz}$, close to the analytically predicted resonance frequency by means of the half-wave dipole

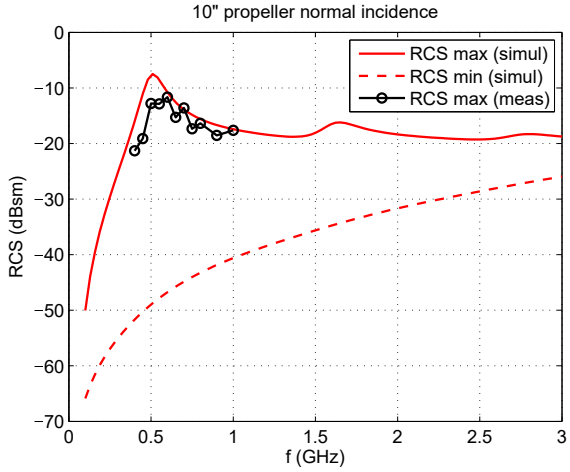

Figure 5. Measured and simulated maximal ($\alpha = 0$) and minimal ($\alpha = 90\,^\circ$) RCS values of the propeller, with respect to the excitation frequency. (Unit is decibel-square meter, dBsm.)

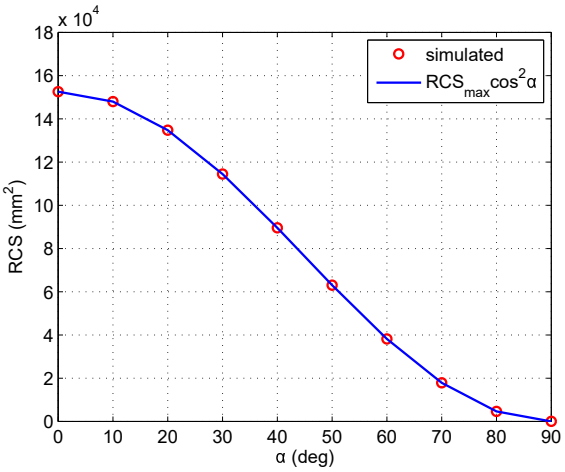

Figure 6. RCS of the propeller at $540\,\mathrm{MHz}$ in function of the polarization angle α. The simulated results perfectly follow the analytic curve proportional to $\cos^2\alpha$.

approximation of the propeller ($f_{\text{halfwave}} = \dfrac{c}{2l} \approx 600\,\mathrm{MHz}$).

IV. Numerical simulation

The goal of the numerical simulations that have been carried out is twofold: first, the $\sigma(f, \alpha)$ function is studied in the viewpoint of the assumed sinusoidal dependence on α; second, the analysis of the frequency dependence of the RCS in the case of maximal ($\alpha = 0$) and minimal ($\alpha = 90\,^\circ$) back-scattered echo of the propeller.

In all simulations, the propeller is modeled by a thin rectangular slab such that its length ($10\,\mathrm{inch}$) and width ($0.9\,\mathrm{inch}$) are close to the dimensions of the propeller (the pitch is neglected). Since the CFRP material can be considered as conductor, the slab is assumed to be made of perfect electrical conductor (PEC) to simplify the electromagnetic model. The scattering phenomenon is modeled by the classical electric field integral equation that is numerically solved by using the method of moments [7]. This method is applied via the commercial software CST Microwave Studio.

The validation of the formula (2) by means of the simulation is shown in Fig. 6. The RCS of the propeller is calculated for 10 values of α and the results appear to perfectly follow the guessed curve proportional to $\cos^2\alpha$.

In Fig. 5, the measured data is compared to the simulations. The latter have been performed in a wider frequency band such that not only can the first significant peak of $\sigma_{\max}(f)$ be seen but a second one around $1.7\,\mathrm{GHz}$ that must correspond to the $l = 3\lambda/2$ mode of the dipole that models the propeller. Let us also note that the ratio of the maximal and minimal RCS tends to decrease as the frequency gets higher, i.e., as the resonant region is being left.

Finally, the effect of the propeller length is analyzed via the simulation shown in Fig. 7. As l increases, the magnitude of the RCS increases as well, whereas the frequency at which $\sigma_{\max}(f)$ is maximal appears to decrease. This can also be explained by the resonant half-wave dipole model of the propeller. Let us emphasize the capability of predicting l based on the spectral analysis of the received echo that is not possible by classical Doppler-based techniques.

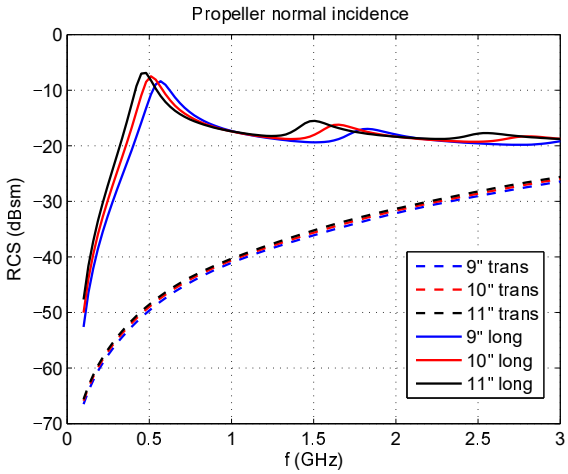

Figure 7. Simulated RCS values of propellers of different lengths l, for transverse ($\alpha = 90\,^\circ$) and longitudinal ($\alpha = 0\,^\circ$) polarization of the incident field. The magnitude and the position of the peak in $\sigma_{\max}(f)$ moves with l as expected.

V. Conclusion, perspectives

The small-sized UAV propellers have low RCS values, however, typically in the UHF band, the RCS strongly depends on the polarization of the incident wave. This phenomenon can be explained via the high conductivity of the CFRP of which the propeller is made and the resonance of the propeller similar to a half-wave dipole antenna. This idea facilitates the measurement of the propeller's RCS in anechoic chamber and the radar detection of UAVs having rotating propellers.

The approach is experimentally validated in anechoic chamber and the measured data are compared to numerical sim-

ulations. The results are in good agreement, justifying the working principle.

The future work is twofold. So far, the case of perpendicular incidence –with respect to the plane of the rotation– has been studied. In the case of arbitrary incidence, not only periodic amplitude modulation, but phase modulation (i.e., Doppler shift) of the backscattered field is expected. The experimental and numerical analysis of theses simultaneous effects will be considered in the future.

In terms of application, signal processing tools are to be developed to exploit the presented effect in real scenarios of UAV detection and tracking by radar. In the typical case of non-cooperative UAVs, the rotation frequency is unknown and can vary during operation. To overcome this, e.g., an adaptive matched filter has to be designed that is able to estimate f_r and track its changes. Utilising these characteristics of the reflected signal at the proper frequency the coherent integration can be extended resulting in more sensitive multirotor UAV detection systems.

ACKNOWLEDGMENT

This work has been partially supported in the frame of the project "Multichannel passive ISAR imaging for military applications (MAPIS) No. B-1359 IAP2 GP" of the European Defence Agency. The authors are grateful to Rudolf Seller for having inspired this work with his ideas and comments.

REFERENCES

[1] A. Moses, M. Rutherford, and K. Valavanis, "Radar-based detection and identification for miniature air vehicles," in *Control Applications (CCA), 2011 IEEE International Conference on*, Sept 2011, pp. 933–940.

[2] M. Kratky and L. Fuxa, "Mini UAVs detection by radar," in *Military Technologies (ICMT), 2015 International Conference on*, May 2015, pp. 1–5.

[3] S. Rea, D. Linton, E. Orr, and J. McConnell, "Electromagnetic shielding properties of carbon fibre composites in avionic systems," *Mikrotalasna revija*, vol. 11, no. 1, pp. 29–32, 2005.

[4] A. Galehdar, P. Callus, and K. Ghorbani, "A novel method of conductivity measurements for carbon-fiber monopole antenna," *Antennas and Propagation, IEEE Transactions on*, vol. 59, no. 6, pp. 2120–2126, June 2011.

[5] J. de Wit, R. Harmanny, and G. Premel-Cabic, "Micro-Doppler analysis of small UAVs," in *Radar Conference (EuRAD), 2012 9th European*, Oct 2012, pp. 210–213.

[6] M. Skolnik, Ed., *Radar Handbook 3rd Edition*. New York: McGraw-Hill, 2008.

[7] R. F. Harrington, *Field computation by moment methods*. New York: Macmillan, 1968.